Experiments on Electron-Beam Measurement : A Review of a Series of Studies Made with the UOP electron Linac and Related Studies

Bulletin of University of Osaka Prefecture
Vol. 42, No. 2, 1993, pp. 193–207.

Experiments on Electron-Beam Measurement: A Review of a Series of Studies Made with the UOP Electron Linac and Related Studies*

Tatsuo TABATA**, Kyue FUKUDA***, Keisuke KAWABATA**, Rinsuke ITO**, Shigeki NAKAMURA***, Ryoichi TANIGUCHI**, Takeyoshi SEIYAMA****, Kunihiko TSUMORI***** and Shuichi OKUDA******

(Received October 30, 1993)

Important experiments on electron-beam measurement, carried out with the linear electron accelerator of University of Osaka Prefecture, are reviewed together with related studies by other authors. Topics treated are measurement of electron-beam characteristics, anomalies in dosimetry and absorbed dose due to heterogeneities, and an application of electron-beam measurement to nondestructive inspection.

1. Introduction

In 1962 a linear electron accelerator (electron linac) with beam energies from 3.5 to 18 MeV was installed at the Radiation Center of Osaka Prefecture[1,2]. The Center was united with University of Osaka Prefecture (UOP) in 1990, and the linac now belongs to Research Institute for Advanced Science and Technology of the university. The topics studied with the UOP linac cover the fields of nuclear physics, nuclear engineering, radiation physics, materials science, radiation chemistry and radiation biology (lists of papers published before 1990 are given in Ref. 3). In the present paper, important experiments on elecetron-beam measurement carried out with the linac are reviewed. Related studies made by other authors are also reviewed briefly.

---

* Dedicated to Dr. Shigeru Okabe on his seventieth birthday. Adapted from part of lectures delivered by one of the authors (T. T.) at the Shanghai University of Science and Technology and Beijing Normal University in 1988 and at the Royal London Hospital in 1989. Some topics treated in Sec. 2 of the present paper were described in an earlier review article: S. Okabe, Oyo Buturi **36**, 860 (1967) (in Japanese).

** Department of Fundamental Science, Research Institute for Advanced Science and Technology
*** Research Center of Radiation, Research Institute for Advanced Science and Technology
**** 6-7 Midorigaokaminamimachi, Kawachinagano
***** Harima Research Laboratories, Sumitomo Electric Industries, Ltd.
****** The Institute of Scientific and Industrial Research, Osaka University

2. Measurement of Electron-Beam Characteristics

As soon as the linac was installed, a group headed by Okabe began a series of studies on the methods to measure characteristics of the electron beam during the time of its usage, i.e., to monitor beam characteristics. The characteristics considered were beam current, beam position in the beam-transport pipe, energy spectrum of the beam, beam profile and beam power at the outside of the accelerator window, and absorbed dose in specimens. During the study of a beam-current monitor, we found an anomalous secondary emission phenomenon.

2. 1 Monitoring of beam current and anomalous secondary emission

To monitor the beam current, we used the secondary electron monitor (SEM; also called secondary emission monitor or secondary emission chamber, SEC) developed by Tautfest and Fechter[4] [a review on the SEM is given in ICRU Report 21 (Ref. 5)].* The monitor consists of aluminum foils placed in the evacuated beam-pipe of the accelerator or in a separate vacuum-chamber. The foils are alternately connected to form emitters and collectors of the secondary electrons generated by the passage of the beam. A bias voltage is applied to one set of the foils. The output from the other set of the foils is fed to a current integrator or an oscilloscope.

At the energies of the UOP linac or at much lower energies, e.g., from 1 to 2 MeV, the foils of the monitor cause a considerable angular spread of the beam. Therefore, we proposed a modified type of the SEM that uses the accelerator output-window as one of the foils[6]. A similar idea was independently published by Taimuty and Deaver[7]. These authors used a separate vacuum-chamber containing a single emitter-foil; the window foils and walls of the chamber acted as the collector..

SEMs were used extensively for measuring the beam intensity of high-energy proton accelerators. Agoritsas and Witkover[8] described a series of tests performed at Fermi National Accelerator Laboratory, Brookhaven National Laboratory and European Center for Nuclear Research (CERN), to improve the stability of the response of SEMs. One of the SEMs tested consisted of a single emitter-foil and nickel mesh-planes with 90% transparency. Ladage[9] measured the energy dependence of the SEM built of thin aluminum foils, for electron energies from about 10 MeV to 5 GeV, and found that it agreed with the theoretical treatment of Aggson[10].

While studying the performance of a SEM, we found an interesting phenomenon, which we called anomalous emission[11]. When the SEM works normally, the output current of the SEM increases with increasing bias voltage, and then reaches a saturated value. The anomalous emission produced a peak superposed on this monotonous

---

* A revised version of the Report, ICRU 35 (1984), does not include a description on the SEM. At the World Congress on Medical Physics and Biomedical Engineering held in Kyoto in 1991, one of the present authors, T. T., met B. Planskoy, who was the author of one of papers on the SEM [Nucl. Instrum. & Methods **24**, 172 (1963)], and asked her about the reason for the disappearance of the description. She answered that fashion might have changed like the way of dressing.

dependence (Fig. 1). The anomalous-emission current showed supralinear dependence on the primary-beam current. Irregularities on the top of the primary-beam pulse were therefore accentuated in the output pulse of the SEM at bias voltages in the anomalous region (Fig. 2). We considered that the cause of the anomalous emission was a modified type of Malter effect[12], i.e., thin-film field emission, due to contamination or the absorbed gas on the surface of the foils.

The appearance of a peak on the current-voltage curve of the SEM does not necessa-

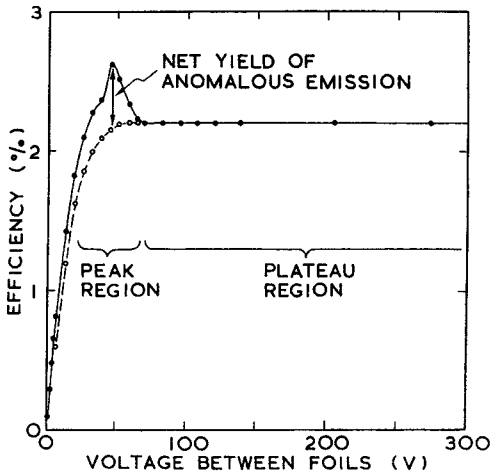

Fig. 1 A peak due to anomalous secondary-emission in the dependence of SEM efficiency on applied voltage. Cited from Ref. 11.

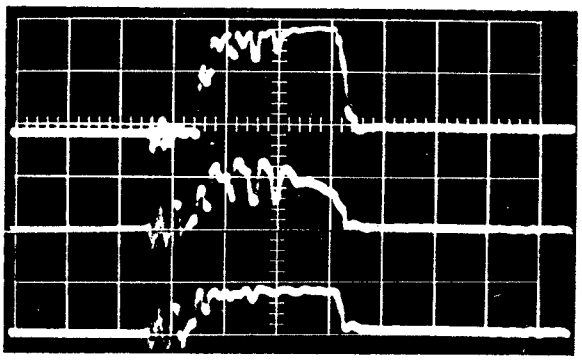

Fig. 2 Pulse output of a SEM compared with the primary-beam pulse (uppermost). Middle, secondary-emission pulse with anomalous emission superposed; lowermost, normal secondary-emission pulse. The large division of the horizontal axis is 2 μsec; that of the vertical axis is 200 mA for the primary beam and 10 mA for the secondary emission. Cited from Ref. 11.

rily indicate the presence of the anomalous emission. Brinkmann and Hellwig[13] observed a slow decrease in the voltage region from 20 to 1000 eV. They explained this by carbon contamination and the energy-dependence of two effects: the backscattering of secondary electrons from the collector foils and the emission of tertiary electrons from the emitter foils by the backscattered secondaries. Ohkuma and Kawanishi[14] found a peak on the current-voltage curve when the accelerator was operated with a short-pulse (20-ns width), high-current (6-A peak) mode. They reported that the secondary-electron current at the peak was stable in contrast to our anomalous emission, and suggested an effect due to strong electric field produced by the primary beam. However, the details of the mechanism have yet to be made clear.

2. 2 Monitoring of beam position

To monitor beam position in the extension pipe of the accelerator, we again used secondary emission. The secondary emission from four pieces of aluminum foil forming a circular aperture gives information on beam position. By making the diameter of the aperture close to that of the beam, the displacement of the beam of about 0.5 mm was easily detected with such a monitor.

Soon after the publication of our paper on the beam-position monitor[15], Peterson[16] published a similar monitor called "thin secondary-emission beam-current and position monitor." With two pairs of semicircular foils, the monitor allowed the beam to be kept on the target to within 0.1 mm. Prudnikov and Toropov[17] described a secondary-emission beam position monitor for a 10-25-MeV medical electron-linac. Their monitor could register the beam-position variations of ± 0.2 mm.

2. 3 Monitoring of energy spectrum

For monitoring the energy spectrum of the electron beam, we developed a method of using elastic scattering of electrons by a thin foil[18]. A chamber with 15-cm diameter and 10-cm height was placed in the beam path. An aluminum foil of 1.8-mg/cm^2 thickness was brought into the beam path by remotely controlled rotation of a rod near the chamber wall. The chamber had an exit port for scattered electrons at 45°. The scattered electrons were analyzed with a double focusing magnet, and detected with a plastic scintillator mounted on a photomultiplier. The direct current from the photomultiplier was amplified and fed to the vertical input of a storage oscilloscope, the horizontal axis of which was swept by magnet current. An example of the energy spectrum observed is shown in Fig. 3. The electron-nuclear elastic peak at the right gives information on the energy spectrum of the primary beam. At the left we see the electron-electron scattering peak. Using this monitor system, we can check the energy spectrum without bending the primary beam by an analyzer magnet.

The use of elastically scattered electrons to measure the energy of the electron beam was reported earlier by Belcher et al[19]. These authors applied the scattering to providing a less intense source of electrons with the same energy as that from a 400-kV Van de Graaff accelerator, thus allowing the energy to be measured with a calibrated solid-state detector. Later Fessenden[20] reported an energy monitor similar to ours. The scatterer of the monitor was a tungsten wire of 0.038 mm diameter, which scat-

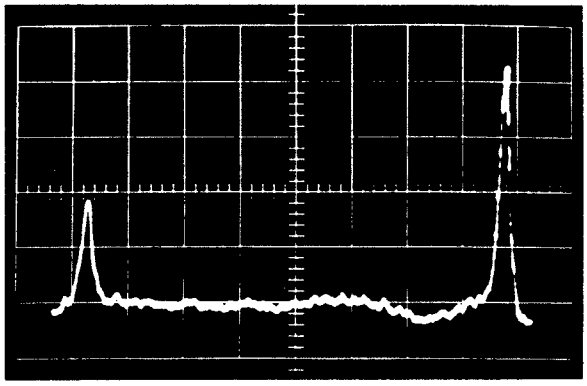

Fig. 3 Example of oscilloscope trace of the energy monitor, about 1.75 MeV/div. Cited from Ref. 18.

tered negligible fraction (about 0.1%) of the primary beam. Piceni and De Vries[21] developed a secondary emission monitor to display the energy spectrum of the beam from a 60-MeV electron linac. The monitor consisted of a grid of ten, 0.1-mm thick, aluminum foils placed perpendicular to the magnetically analyzed beam. Measurement of the secondary-emission current for each strip separately yielded the energy spectrum of the beam.

2. 4 Monitoring and measurement of beam profile

Using scattered electrons again, we developed a method to monitor the current profile of the scanning electron-beam[22]. This time the scatterer was the output window of the accelerator. A multi-probe detector collected the electrons scattered in the direction of 40°, and the beam profile was displayed on a storage oscilloscope. In Fig. 4, a profile observed by collecting scattered electrons is compared with a profile observed by collecting the primary beam directly, for the same operating conditions of the linac.

We developed also a method to measure beam profile at the outside of the accelerator window by the use of secondary electrons[23]. The probe was made of an enamel-coated copper wire or a small and thin aluminum disk covered by thin insulating film, and was carried by a sweeping device. An example of beam profiles at the scanning-beam port measured with the disk probe is shown in Fig. 5(a). In the UOP linac the scanner-coil current is swept with a frequency of 6 cycles per second, and the repetition rate of beam pulse is variable from about 10 to 100 pulses per second. At low repetition rates of beam pulse, therefore, occasional matching of pulse-repetition rate to an integer- or half-integer-multiple of scanning frequency causes a beam profile with several peaks as shown in Fig. 5(b). For irradiation of long duration, such matching is expected to be destroyed easily by a slight change of pulse-repetition rate. Strangely, however, the occurrence of profiles with several peaks was rather common at low pulse-repetition rates. Later, it was found that the noise caused by the ignition of the pulse-forming network was re-triggering the wave-form generator for the scanner-coil current to repeat the same relative phase between the scanning and beam pulses. We

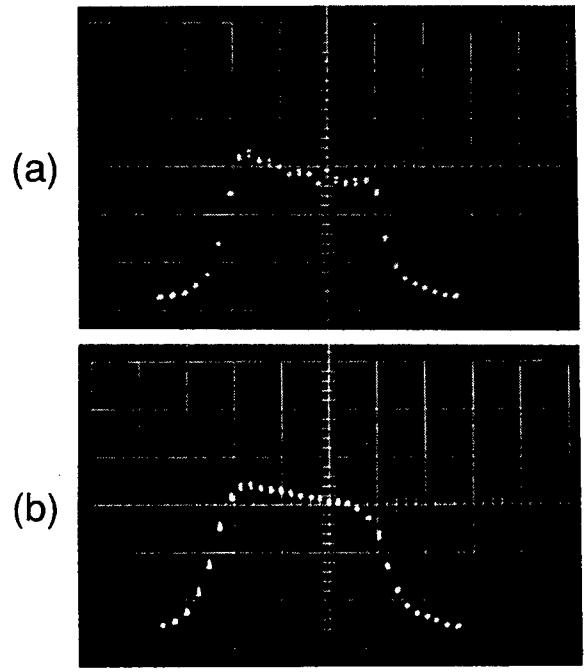

Fig. 4 (a) Profile of a scanning electron-beam, observed by collecting scattered electrons. (b) Corresponding profile at the irradiation position. The large division of the horizontal axis represents a spatial distance of 10 cm. Cited from Ref. 22.

then modified the wave-form generator not to be triggered by the noise.

Balsamo *et al.*[24] described a device to monitor beam position and profile in the transport pipe of a 400-MeV electron-positron linac. The monitor consisted of two tungsten wires of 1-mm diameter at right angle and moving simultaneously through the beam. The secondary-emission current from the wires yielded beam profiles in x and y directions. Prudonikov *et al.*[25] described a beam profile monitor made of a rotating copper-wire of 50-μm diameter. Hortig[26] showed that a single rotating-wire having the form of the more rigid half of an ellipse was capable of delivering a full two-dimensional display of the beam profile.

More recently we developed a new beam profile monitor for scanning electron beams[27]. A multi-probe detector system consisting of 64 copper bars is placed at the irradiation port by remote control when measurement is necessary. The bars collect the primary electrons. The charges collected are stored by capacitors. The voltages over the capacitors are converted to optical signals and transmitted to the control room of the linac. A microcomputer receives the signals and translates them into digital values. Finally beam profile is shown on the display unit of the microcomputer.

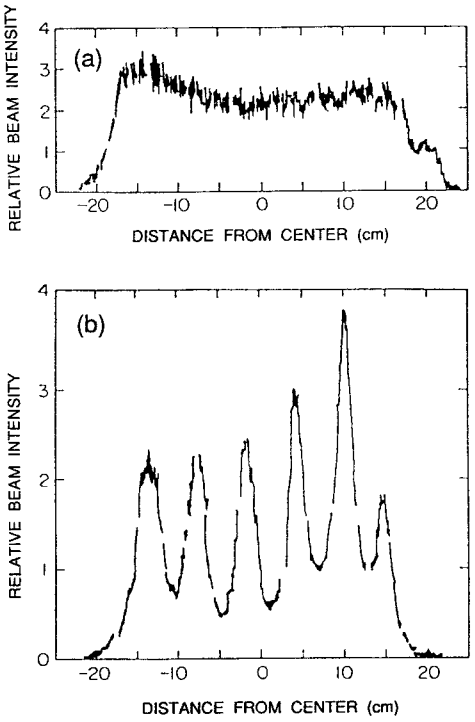

Fig. 5 Beam profiles at the scanning-beam port of the linac measured with a secondary emission probe carried by a sweeping device; (a) at high repetition rate of beam pulse, (b) at low repetition rate of beam pulse. Cited from Ref. 23.

2. 5 Measurement of beam power and absorbed dose: Calorimetry

To measure beam power at the outside of our linac, we prepared a twin water-flow calorimeter (a compensation calorimeter)[28–30]. Equal flows of water were passed continuously through two identical chambers (not by series connection), and the output temperatures of the two water streams were balanced with a heater in the dummy side. The performance of the calorimeter was tested for electron beams of energies from 1.0 to 1.8 MeV provided by a Van de Graaff type accelerator and those of energies from 5 to 20 MeV provided by a linac; the latter was an accelerator installed at Japan Atomic Energy Research Institute before our linac. The results of the test were satisfactory in the range of beam powers from 20 to 4000 W.

We developed another type of twin calorimeter to measure the energy absorbed in specimens of different thicknesses (a differential calorimeter)[31]. Two aluminum collectors in an evacuated chamber were irradiated by scanning electron beams. The difference of the voltages from the two thermocouples, each attached to one of the collectors, was initially confirmed to be essentially zero. Then a specimen was placed in front of one of the collectors. From the slope of the rise of the temperature difference during irradiation, absorbed dose-rate was determined. Integral depth-dose curves

of 1.0- to 1.8-MeV electrons in aluminum were measured by the calorimeter, showing good agreement with the curves obtained from Nakai's ionization measurement[32].

Gunn wrote a series of reviews[33)-35)] on radiometric calorimetry for the period from 1949 to 1975, and listed a total of about 770 references, in which our studies mentioned above are included. A more recent review of calorimetric dosimetry systems is found in a book authored by McLaughlin *et al.*[36]

3. Anomalies in Dosimetry and Absorbed Dose

3. 1 Dosimetry with mica

We studied to use sheets of natural mica for dosimetry[37]. A collimated electron beam from the linac was incident on the absorber-dosimeter system. The system consisted of a mica sheet sandwiched between two semicylindrical aluminum blocks, and was placed so that the axis of the electron beam was on the plane of the mica sheet. After exposure to electrons, the mica sheet was heated to a temperature of 760 ℃ for an hour. Then the part of the sheet exposed to doses less than a value given by a calibration curve turned into silvery white and opaque. On the other hand, the part exposed to doses higher than that value remained transparent. This was caused by the radiation induced increase of resistance of mica against thermal descomposition.

This phenomenon enabled us to map the isodose curves of electrons in the aluminum absorber. The central axis depth–dose curve obtained from the isodose curves showed however an unexpected minimum at a small depth (Fig. 6). We then studied the cause of this minimum. What we found constitutes the next topic.

3. 2 Dose anomalies due to heterogeneities

We found that the geometry of the absorber-dosimeter system was responsible for the dose minimum described above. In the geometry used, narrow gaps are produced between the dosimeter and the absorber. Though their width is negligible in a macroscopic scale, the gaps cause a streaming effect of electrons. We measured the dose distribution near the surface of the absorber by changing the width of the gaps with spacers and by changing the angle of incidence of the beam[38]. These changes produced variation of doses near the surface, which indicated how the streaming of electrons affects the measurement of the depth–dose curve. Earlier Dutreix and Dutreix[39] also discussed the effect of the air gap between the absorber and the film dosimeter.

We can explain the streaming effect by a simple model. There are two components of dose that contribute to the dose measured by the film dosimeter (Fig. 7). Component I comes from the electrons initially incident on the dosimeter, and component II, from the electrons initially incident on the absorber. The electrons initially incident on the absorber and then scattered toward the dosimeter impinge on the dosimeter after passing a certain length in the gap. For a wider gap, the average value of this length is larger. Then the rise of component II is slower, and a larger dip occurs on

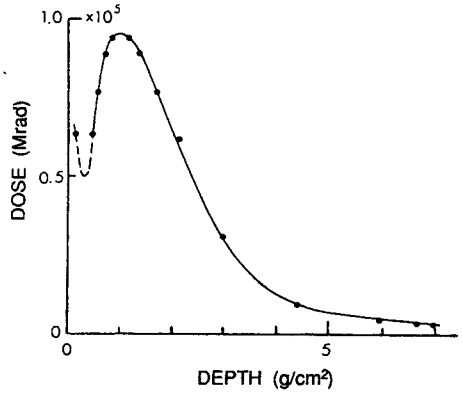

Fig. 6 Central axis depth–dose curve of 15-MeV electrons incident on aluminum absorber, measured with a mica dosimeter. Cited from Ref. 37.

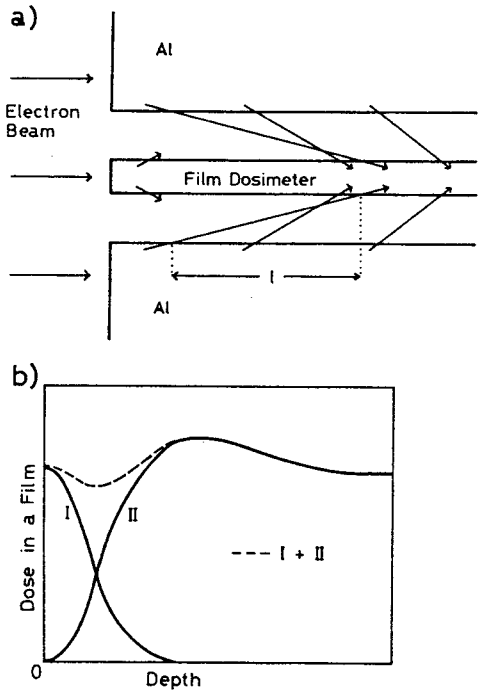

Fig. 7 (a) Simplified model of electron streaming through air gaps between aluminum absorbers and a film dosimeter; l denotes the streaming length of an electron. (b) Dose component I is due to electrons initially incident on a film dosimeter, and component II is due to electrons initially incident on aluminum absorbers. Cited from Ref. 38.

the dose near the surface.

We see the effect of streaming also in the work done by Humphreys *et al.*[40] They used the stack method and the wedge method in measuring depth-dose curves of electrons. In the former method, disks of the absorber material and sheets of a dye-film dosimeter were alternately assembled. In the latter method, a strip of the dosimeter was obliquely sandwiched between the absorber pieces. The depth-dose curves measured by the wedge method showed an anomaly near the surface, but the authors did not give clear explanation for this.

From the study of the streaming effect, we considered that the heterogeneities of materials irradiated by electron beams might show unexpected anomalies of the absorbed dose. To check this possibility, we studied the dose profiles of electrons after passing model heterogeneities[41].

One of the model heterogeneity studied was the edge of a thin aluminum plate. The aluminum plate and a film dosimeter were placed horizontally with a gap between them. Viewed from the top, half the area of the dosimeter was covered by the aluminum plate. A broad beam of electrons was incident on the plate-dosimeter assembly. The energy of the electrons used was 10 MeV, so that almost all the electrons incident on the plate passed through it, suffering only a small amount of energy loss. The electrons transmitted through the plate and those directly incident on the dosimeter gave almost the same dose to the dosimeter. However, within a small region just below the edge of the plate, we saw a dose perturbation due to the discontinuity in the density of the material traversed by the electrons (Fig. 8). A similar problem was studied earlier by Markus[42] and recently by Mehta *et al.*[43] The latter authors measured the dose perturbation under the edge of acrylic blocks with a red-acrylic dosimeter, and compared the results with Monte Carlo calculations.

Other model heterogeneities we studied were a needle and a silk suture often irradiated for sterilization. In the case of the needle, we saw a large modification of about 40% from a uniform dose profile (Fig. 9). These results indicate that the check of uniformity in absorbed dose is imperative when we irradiate heterogeneous samples in a multilayer configuration by electron beams.

4. An Application of Electron Beam Measurement: Nondestructive Inspection with Electron Beams

Streaming and other effects that electron beams suffer in passing heterogeneous materials are considered to offer a possible method of nondestructive inspection. We then studied the detection of small voids in solids by observing electrons with initial energy of 10 MeV transmitted through samples, with the aid of magnetic spectrometer (transmission spectrometry)[44]. Earlier Boiko *et al.*[45] made a similar study using electrons of energies from 3 to 5 MeV, but without energy analysis.

The analyzed electron beam from the linac was collimated and passed through a sample. The sample was made of three layers of ceramics. The middle layer consisted

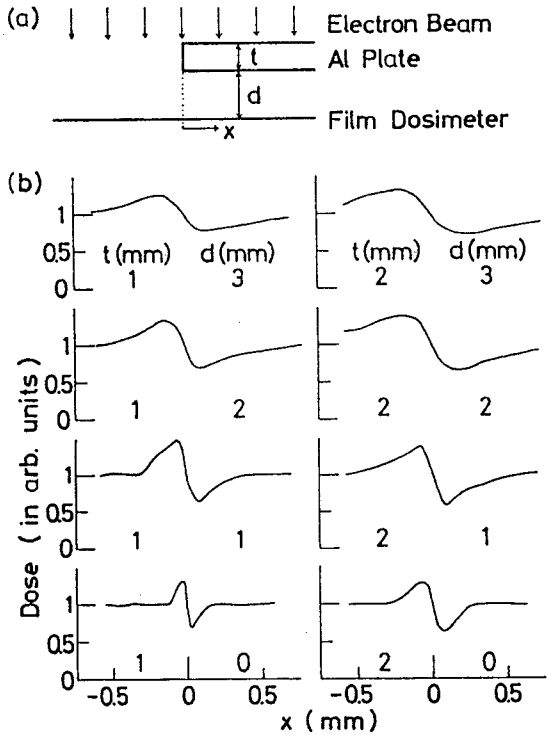

Fig. 8 Measurement of dose perturbation due to model heterogeneity; (a) experimental arrangement, (b) dose profile due to a broad beam of 10-MeV energy. Cited from Ref. 41.

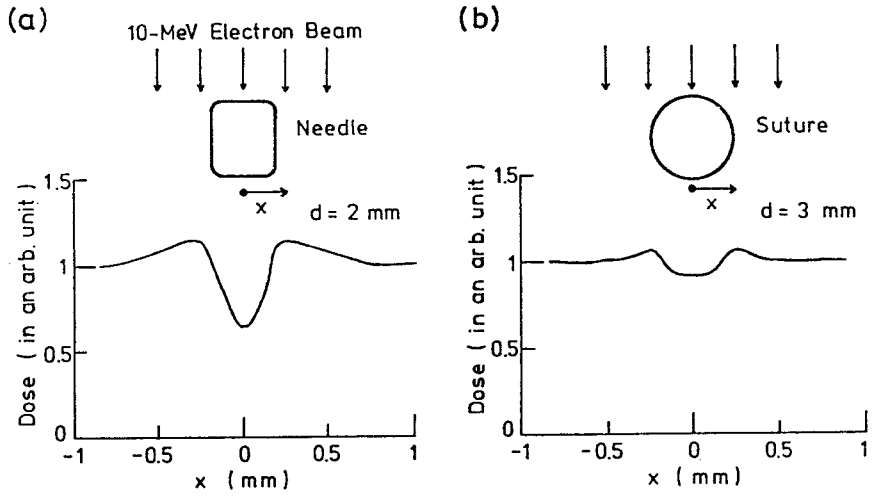

Fig. 9 Dose profiles of 10-MeV electrons after penetration through (a) a needle and (b) a silk suture. The symbol *d* denotes the distance of the film dosimeter from the bottom of the sample. Cited from Ref. 41.

of two pieces, between which a narrow cavity was left as a model defect (see the inset to Fig. 10). The plastic scintillator of the energy monitor, described in Sec. 2.2, served as the detector of magnetically analyzed electrons. Figure 10 shows the energy spectra of electrons transmitted through samples with and without a cavity. From such differences in the spectra, it is possible to find voids in a material layer.

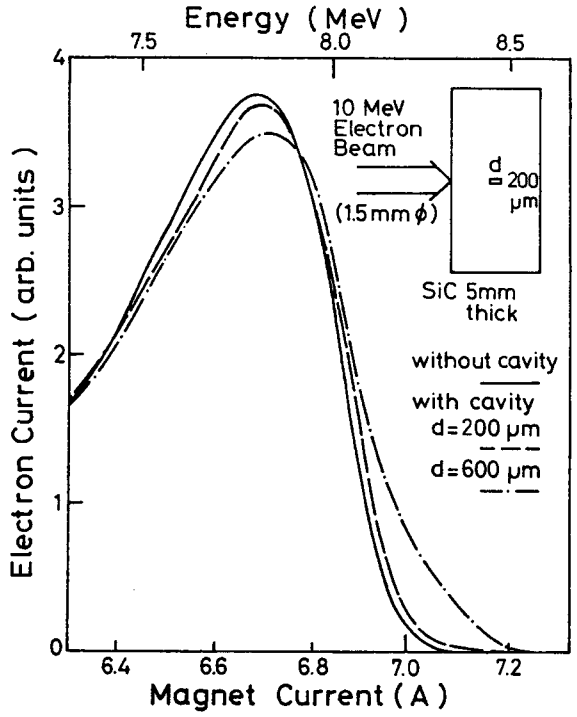

Fig. 10 Energy spectra of electrons transmititted through SiC samples with and without a cavity. The inset shows the configuration of the electron beam and the sample (not to scale). Cited from Ref. 44.

Figure 11 shows the energy spectrum of electrons transmitted through a sample containing a different type of model defect. The sample was made of two pieces of SiC plates of 5-mm thickness, in touch with each other at one of their smooth side surfaces (see the inset to Fig. 11). Peak *a* is due to the electrons that passed through the full thickness of the plates, and peak *b* is due to the electrons that streamed through the model defect without suffering energy loss. This result shows that a void that is long in the direction of the beam might easily be detected by the transmission electron spectrometry, even when its sizes in the other directions are extremely small.

Figure 12 shows the result of study to detect model defects in the form of grooves made in the surface of a ceramic plate of 3-mm thickness. Electrons were incident from the surface with the grooves. The magnet current was fixed at the value corresponding to the middle of the high-energy side of the peak on the energy spectrum of the electrons transmitted through the region of the sample without defects, and the

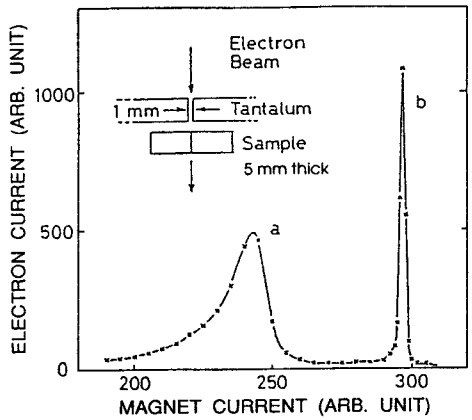

Fig. 11 Energy spectrum of electrons transmitted through a sample with a long and thin model-defect. The sample was made of two pieces of SiC plates of 5-mm thickness, in touch with each other at one of their smooth side surfaces (see the inset). Peak *a* is due to the electrons that passed through the full thickness of the plates, and peak *b* is due to the electrons that streamed through the model defect without suffering energy loss.

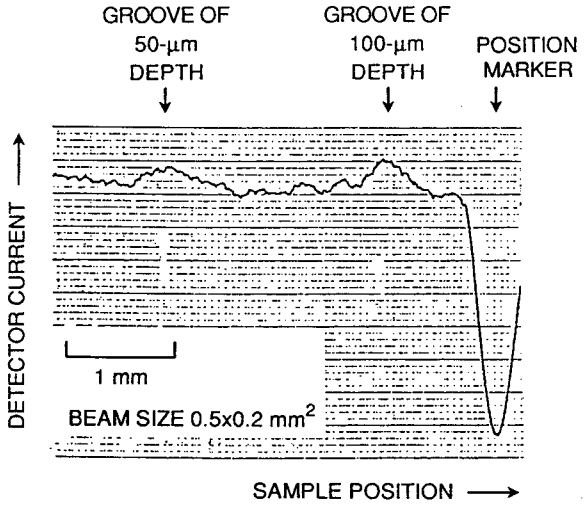

Fig. 12 Signal from the magnetic spectrometer when a ceramic-plate sample with model defects of known sizes was swept through the beam. The model defects were grooves of 50- and 100-μm depths in the electron-incidence surface, and the thickness of the sample was 3 mm. A large dip of signal at the right is due to a thin wire attached to the sample as a position marker.

sample was swept perpendicularly to the beam. The smallest groove that could be observed was 50 μm in depth. A large dip of signal at the right of the figure is due to a thin wire attached to the sample as a position marker. The defects that are apt to be introduced into ceramics in production process are considered to have a size of about 5-μm diameter. To find such defects, therefore, a sensitivity ten times higher than that we have achieved would be necessary.

References

1) S. Okabe, K. Tsumori, T. Tabata, K. Kawabata, K. Fukuda, R. Ito, S. Nakamura, T. Azuma and K. Kimura, Ann. Rep. Radiat. Center Osaka Prefect., **3**, 47 (1962).
2) S. Okabe, K. Tsumori, K. Fukuda, T. Tabata, K. Kawabata, R. Ito, S. Nakamura, T. Azuma and K. Kimura, Ann. Rep. Radiat. Center Osaka Prefect., **3**, 54 (1962).
3) K. Fukuda and T. Tabata, "Present Status and Results of the UOP Linear Electron Accelerator", Report, Res. Inst. Adv. Sci. Tech., Univ. Osaka Prefect. (1990).
4) G. W. Tautfest and H. R. Fechter, Rev. Sci. Instrum., **26**, 229 (1955).
5) ICRU, "Radiation Dosimetry: Initial Energies between 1 and 50 MeV", Report 21 (1972).
6) S. Okabe, T. Tabata and R. Ito, Rev. Sci. Instrum., **32**, 1347 (1961).
7) S. I. Taimuty and B. S. Deaver Jr., Rev. Sci. Instrum., **32**, 1098 (1961).
8) V. Agoritsas and R. L. Witkover, IEEE Trans. Nucl. Sci., **NS-26**, 3355 (1979).
9) A. Ladage, "Energy Dependence of Secondary Emission Monitors between 10 MeV and 5 GeV", Report DESY-65/16, Deutsches Elektronen-Synchrotron (1965).
10) T. L. Aggson, Report LAL-1028, Laboratoire de l'Accélérateur Linéaire, Orsay, France (1962).
11) S. Okabe, T. Tabata and R. Ito, Nucl. Instrum. & Methods, **26**, 349 (1964).
12) L. Malter, Phys. Rev., **50**, 48 (1936).
13) E. Brinkmann and G. Hellwig, Nucl. Instrum. & Methods, **48**, 163 (1967).
14) J. Ohkuma and M. Kawanishi, Nucl. Instrum. & Methods, **211**, 547 (1983).
15) S. Okabe and T. Tabata, Rev. Sci. Instrum., **36**, 97 (1965).
16) G. A. Peterson, Rev. Sci. Instrum., **36**, 708 (1965).
17) I. A. Prudnikov and A. S. Toropov, Nucl. Instrum. & Methods, **92**, 359 (1971).
18) S. Okabe, T. Tabata and K. Tsumori, Rev. Sci. Instrum., **37**, 309 (1966).
19) R. L. Belcher, J. M. McGarrity and J. Silverman, Trans. Am. Nucl. Soc., **7**, 321 (1964).
20) T. J. Fessenden, Rev. Sci. Instrum., **43**, 1090 (1972).
21) H. A. L. Piceni and C. De Vries, Nucl. Instrum. & Methods, **51**, 87 (1967).
22) S. Okabe, K. Tsumori and T. Tabata, Rev. Sci. Instrum., **41**, 1537 (1970).
23) S. Okabe, T. Tabata and K. Tsumori, Jpn. J. Appl. Phys., **5**, 68 (1966).
24) E. P. B. Balsamo, C. Guaraldo and R. Scrimaglio, Nucl. Instrum. & Methods, **55**, 339 (1967).
25) I. A. Prudnikov, A. S. Toropov, Y. F. Chichika and I. V. Khokhrya, Nucl. Instrum. & Methods, **114**, 101 (1974).

26) G. Hortig, Nucl. Instrum. & Methods, **30**, 355 (1964).
27) R. Taniguchi, K. Kawabata and K. Yamashita, Ann. Rep. Radiat. Center Osaka Prefect., **28**, 17 (1988).
28) S. Okabe, K. Tsumori, K. Kawabata and K. Fukuda, Ann. Rep. Radiat. Center Osaka Prefect., **2**, 43 (1961).
29) S. Okabe, K. Tsumori and K. Kawabata, Ann. Rep. Radiat. Center Osaka Prefect., **3**, 58 (1962).
30) S. Okabe, K. Tsumori and K. Kawabata, Oyo Buturi, **33**, 312 (1964) (in Japanese).
31) S. Okabe, T. Tabata and K. Tsumori, Ann. Rep. Radiat. Center Osaka Prefect., **10**, 45 (1969).
32) Y. Nakai, Jpn. J. Appl. Phys., **2**, 743 (1963).
33) S. R. Gunn, Nucl. Instrum. & Methods, **29**, 1 (1964).
34) S. R. Gunn, Nucl. Instrum. & Methods, **85**, 285 (1970).
35) S. R. Gunn, Nucl. Instrum. & Methods, **135**, 251 (1976).
36) W. L. McLaughlin, A. W. Boyd, K. H. Chadwick, J. C. McDonald and A. Miller, "Dosimetry for Radiation Processing" Taylor and Francis, London (1989).
37) K. Fukuda, S. Nakamura, Y. Satoh, T. Tabata and S. Okamoto, Nucl. Instrum. & Methods, **172**, 487 (1980).
38) S. Okuda, K. Fukuda, T. Tabata and S. Okabe, Nucl. Instrum. & Methods, **200**, 443 (1982).
39) J. Dutreix and A. Dutreix, Ann. New York Acad. Sci., **161**, 33 (1969).
40) J. C. Humphreys, S. E. Chappell, W. L. McLaughlin and R. D. Jarrett, "Measurement of Depth-Dose Distributions in Carbon, Aluminum, Polyethylene, and Polystyrene for 10-MeV Incident Electrons", Report NBSIR 73-413, Ntl. Bur. Stand. (1973).
41) S. Okuda, S. Nakamura, T. Tabata, K. Fukuda, T. Seiyama and S. Okabe, Radiat. Phys. Chem., **26**, 679 (1985).
42) B. Markus, Ann. New York Acad. Sci., **161** 282 (1969).
43) K. K. Mehta, R. Chu and G. VanDyk, Radiat. Phys. Chem., **31**, 425 (1988).
44) S. Okuda, T. Tabata and T. Seiyama, Jpn. J. Appl. Phys., **25**, L848 (1986).
45) V. I. Boiko, V. V. Evstigneev, B. A. Kononov and A. L. Plotnikov, Defektoskopiya, **1977**, 94 (1977).